ELSEVIER

PII: S0032-3861(97)00100-6

Polymer Vol. 38 No. 22, pp. 5579–5586, 1997

0032-3861/97/$17.00 + 0.00

Determination of relaxation and diffusion activation energies during dissolution of latex film using *in situ* fluorescence technique

Ş. Uğur and Ö. Pekcan*
Department of Physics, Istanbul Technical University, 80626, Maslak, Istanbul, Turkey
(Received 18 October 1996; revised 2 December 1996)

In situ, real-time steady state fluorescence measurements used for studying the dissolution of polymer films. These films were formed from pyrene labelled poly(methyl methacrylate) (PMMA) latex particles, sterically stabilized by polyisobutylene. Annealing was performed above the T_g at 180°C during 1 h for film formation. Desorption of pyrene labelled PMMA chains was monitored in real time by the change in pyrene fluorescence intensity. Dissolution experiments were performed in toluene and a toluene/heptane mixture at elevated temperatures. Relaxation (k_0) and diffusion (D) parameters were measured and found to be around 10^{-2} mg cm^{-2} min^{-1} and 10^{-11} cm^2 s^{-1}, respectively. Using these parameters, relaxation (ΔE_{k0}) and diffusion (ΔE_D) activation energies were calculated and found to be 11.36 and 24.38 kcal mol^{-1} and were attributed to the side-chain and backbone motions, respectively. © 1997 Elsevier Science Ltd.

(Keywords: fluorescence; latex film; dissolution)

INTRODUCTION

The mechanism of polymer film dissolution is very different to, and more complicated than, small molecule dissolution. The dissolution of small molecules can be explained by simple diffusion laws[1] and a unique diffusion rate. However, polymeric films dissolve mainly in three different stages: (i) solvent penetration, (ii) polymer relaxation, and (iii) diffusion of polymer chains into the solvent reservoir. A schematic representation of these three sequential steps for the dissolution of a polymer film is presented in *Figure 1*. In the first stage, the penetration distance of solvent molecules mainly depends on free volume, which in turn depends on the flexibility of the chains, backbone and side groups, as well as the thermal history of the polymer. These first solvent molecules act as a plasticizer, and as a result these regions of the film start to swell. In the second stage, a gel layer is created by the relaxing polymer chains. This transition layer is composed of both polymer chains and solvent molecules. If the solvent–polymer interactions are more dominant than the polymer–polymer interactions, maximum swelling is obtained. This is the case when a good solvent is used during dissolution of a polymer film. In the last stage, chain disentanglement takes place, then chains separate from the bulk and diffuse into the solvent.

Polymer dissolution has been studied both theoretically and experimentally. Ueberreiter and coworkers[2] were the first to monitor dissolution of polymers using refractometry and optical microscopy. With this technique the structure of the gel layer was studied as a function of temperature and molecular weight of the polymer. This technique was then improved by designing a critical angle illumination microscope[3]. Poly(methyl methacrylate) (PMMA) film dissolution was studied using laser interferometry by varying the molecular weight and solvent quality[4]. Limm *et al.*[5] modified the interferometric technique and studied the dissolution of fluorescence labelled PMMA films. By monitoring the intensity of fluorescence from the film along with the interferometric signal, the solvent penetration rate into the film and the dissolution are measured simultaneously. Fluorescence quenching and depolarization methods have been used for penetration and dissolution studies in solid polymers[6–8]. A real-time, non-destructive method for monitoring small molecule diffusion in polymer films was developed[8–12]. This method is essentially based on the detection of excited fluorescence dyes desorbing from a polymer film into a solution in which the film is placed. Recently, we have reported a steady state fluorescence (SSF) study on the dissolution of both annealed latex film and PMMA discs using real-time monitoring of fluorescence probes[13,14].

Dispersion of polymer colloid particles with a glass transition temperature, T_g, above the drying temperature is called high-T latex dispersion. These particles remain essentially discrete and undeformed during the drying process. The mechanical properties of high-T powder films can be enhanced, by annealing after all the solvent has evaporated. This process is called sintering and is an important aspect of latex coating technology. In this work we study the dissolution of films formed from high-T latex particles labelled with pyrene (P) dye molecules[15]. These particles have two components: the major part, PMMA, comprises 96 mol% of the material, and the

* To whom correspondence should be addressed

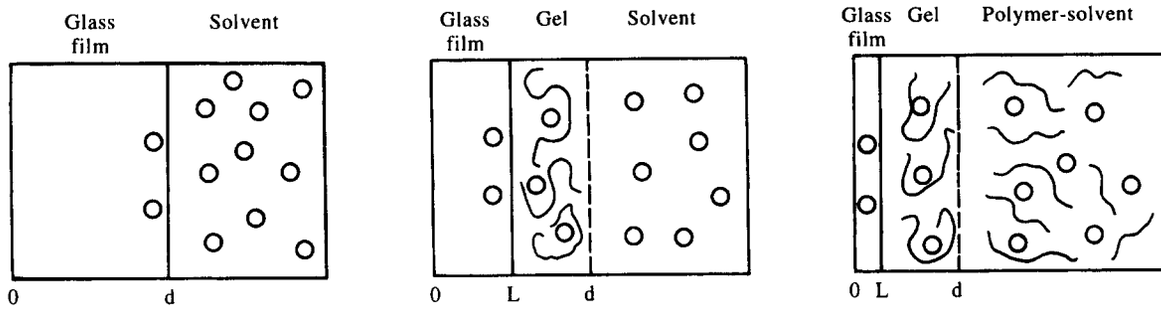

Figure 1 Schematic representation of polymer film dissolution stages; d is the film thickness and L is the position of the advancing gel front

minor component, polyisobutylene (PIB) (4 mol%), forms an interpenetrating network through the particle interior[16,17], highly soluble in certain hydrocarbons. A thin layer of PIB covers the particle surface and provides colloidal stability by steric stabilization. Film samples are prepared by annealing latex powders above the T_g, at 180°C, for 1 h. Toluene and toluene/heptane mixtures are used as dissolution agents. Two sets of *in situ* SSF experiments are performed for real-time monitoring of the dissolution processes. In the first set, dissolution experiments are performed in toluene at temperatures between 15 and 40°C. In the second set of experiments, films are dissolved in toluene/heptane mixture at temperatures between 25 and 65°C. Here, our goal is to slow down the solubility by adding heptane to the system. The dissolution temperature is then increased to determine the dissolution activation energy in the high temperature region. Dissolution experiments are designed so that dye labelled PMMA chains, desorbed from the swollen gel, are detected by the SSF method. In order to do that, direct illumination of the film sample is avoided during the *in situ* dissolution experiment. Our main interest in the present work is to create mechanically strong films by annealing and then study the dissolution process at various temperatures to determine the relaxation and diffusion activation energies.

THEORETICAL CONSIDERATION

Various mechanisms and various mathematical models have been considered for the polymer dissolution. Tu and Quano[18] proposed a model which included polymer diffusion in a liquid layer adjacent to the polymer and moving of the liquid/polymer boundary. The key parameter for this model was the polymer dissociation rate, defined as the rate at which polymer chains desorb from the gel interface. Lee and Peppas[19] extended this model for films to the situation of the polymer dissolution rate where gel thickness was found to be proportional to t (time)$^{1/2}$. A relaxation controlled model was proposed by Brochardt and de Gennes[20] where, after a swelling gel layer was formed, desorption of polymer from the swollen bulk was governed by the relaxation rate of the polymer stress. This rate was found to be of the same order of magnitude as the reptation time. The dependencies of the radius of gyration and the reptation time on polymer molecular weight and concentration were studied, using a scaling law[21], based on the reptation model.

In this paper, we employed a simpler model developed by Enscore *et al.*[22] to interpret the results of polymer swelling and dissolution experiments. This model includes case I and case II diffusion kinetics.

Case I or Fickian diffusion

The solution of a unidirectional diffusion equation for a set of boundary conditions is cited by Crank[1]. For a constant diffusion coefficient, D, and fixed boundary conditions, the sorption and desorption transport in and out of a thin slab is given by the following relation:

$$\frac{M_t}{M_\infty} = 1 - \frac{8}{\pi^2}\sum_{n=0}^{\infty}\frac{1}{(2n+1)^2}\exp\left(\frac{-(2n+1)^2 D\pi^2 t}{d^2}\right) \quad (1)$$

Here, M_t represents the amount of materials absorbed or desorbed at time t, M_∞ is the equilibrium amount of material, and d is the thickness of the slab.

Case II diffusion

Case II transport mechanism is characterized by the following steps. As the solvent molecules enter into the polymer film, a sharp advancing boundary forms and separates the glassy part of the film from the swollen gel (see *Figure 1b*). This boundary moves into the film at a constant velocity. The swollen gel behind the advancing front is always at a uniform state of swelling. Now, consider a cross-section of a film with thickness d, undergoing case II diffusion as in *Figure 1*, where L is the position of the advancing sorption front, C_0 is the equilibrium penetrant concentration, and k_0 (mg cm^{-2} min^{-1}) is defined as the case II relaxation constant. The kinetic expression for the sorption in the film slab of an area A is given by

$$\frac{dM_t}{dt} = k_0 A \quad (2)$$

The amount of penetrant, M_t, absorbed in time t will be

$$M_t = C_0 A(d - L) \quad (3)$$

After equation (3) is substituted into equation (2) the following relation is obtained

$$\frac{dL}{dt} = -\frac{k_0}{C_0} \quad (4)$$

It can be seen that the relaxation front, positioned at L, moves towards the origin with a constant velocity, k_0/C_0. The algebraic relation for L, as a function of time

t, is described by equation (5):

$$L = d - \frac{k_0}{C_0} t \tag{5}$$

Since $M_t = k_0 A t$ and $M_\infty = C_0 A d$, the following relation is obtained:

$$\frac{M_t}{M_\infty} = \frac{k_0}{C_0 d} t \tag{6}$$

EXPERIMENTAL

Material and film preparation

Pyrene (P)-labelled PMMA–PIB latex particles were prepared separately in a two-step process, in which MMA in the first step was polymerized to low conversion in cyclohexane in the presence of PIB containing 2% isoprene units to promote grafting. The graft copolymer so produced served as dispersant in the second stage of polymerization, in which MMA was polymerized in a cyclohexane of the copolymer. Details are published elsewhere[15]. A stable spherical high-T dispersion of polymer particles was produced, ranging in radius from 1 to 3 μm. A combination of ^{1}H nuclear magnetic resonance and ultraviolet analysis indicated that these particles contain 6 mol% PIB and 0.037 mmol P groups per gram of polymer. We refer to these particles as P. (The particles were prepared in M. A. Winnik's Laboratory, University of Toronto, Toronto, Canada.)

To prepare the latex film the P particles were dispersed in heptane in a test-tube. The solid content was equal to 0.24%. Film samples were prepared from this dispersion, by placing numbers of drops on $3 \times 0.8\,cm^2$ glass plates and allowing the heptane to evaporate. The liquid dispersion from the droplets covered the whole surface area of the plate and remained there until the heptane evaporated. Samples were weighed before and after the film casting to determine the film thickness. The average film thicknesses were around 10 μm for the first and second experimental sets. The average size of the particles was taken as 2 μm to estimate the number of layers or the thickness of film samples. The films were annealed in an oven for 1 h above the T_g at 180°C maintained within ± 2°C during annealing.

For dissolution experiments two different sets of experiments were prepared; in the first set, film samples were dissolved in pure toluene at 15, 20, 25, 30, 35 and 40°C. In the second set of experiments a toluene/heptane (4/1) mixture was used for the dissolution experiments and samples were kept at 25, 30, 35, 40, 45, 50, 55, 60 and 65°C during the dissolution processes. The solvents were purchased from Merck Co. (Spectroscopically pure grade) and used as received. Since toluene is a good solvent for PMMA, heptane is introduced into the mixtures to slow down the dissolution process in the second set of experiments.

Instrument for dissolution

Dissolution experiments were performed in a 1.0×1.0 cm quartz cell equipped with a temperature controller. This cell was placed in the spectrofluorimeter, and fluorescence emission was monitored at a 90° angle so that the film samples were not illuminated by the excitation light. Film samples were attached at one side of the quartz cell filled with the toluene/heptane mixture. The cell was then illuminated with 345 nm excitation light. The fluorescence intensity of P, I_p, was monitored during the dissolution process at 375 nm using the 'time drive' mode of the spectrofluorimeter. Emission of P-labelled polymer chains was recorded continuously at 375 nm as a function of time until there was no observable change in intensity. The dissolution cell and the film position is depicted in *Figure 2*. Two different sets of dissolution experiments were run; in the first one, 10 μm film samples were dissolved with pure toluene. In the second set, the toluene/heptane (4/1) mixture was used to dissolve 10 μm film samples.

RESULTS AND DISCUSSION

It has been observed that mechanically rigid and transparent film can be formed by annealing high-T latex particles at 180°C for 1 h[23–28]. These observations are made by using a direct energy transfer method in conjunction with the SSF techniques[25] and/or by a direct fluorescence method[26–28]. Below 180 at 130°C annealing the latex film for 1 h causes the healing process at the particle–particle junction where polymer chains relax across the junction surface. During this time at 130°C chains move at least half way across the junction surface[23]. Above this temperature particle boundaries start to disappear and, consequently, the latex film becomes mechanically strong as a result of annealing[25,28]. To illustrate these findings, scanning electron micrographs of latex film before and after annealing at 180°C for 1 h are presented in *Figure 3*. *Figure 3a* shows high-T latex particles in a powder form. By annealing the latex film at 180°C one can obtain an almost transparent film (*Figure 3b*).

Relaxation and diffusion parameters

The P-group labelled polymer chains were excited at 345 nm during *in situ* dissolution experiments, and the variation in fluorescence emission intensity, I_p, was monitored with the time drive mode of the spectrofluorimeter. The fluorescence P intensity, I_p, is plotted as a function of 'dissolution time' for film samples dissolved in toluene (*Figure 4*) at elevated temperatures. One can observe that as the dissolution temperature increases, film samples start to dissolve at early times. These curves reached a plateau almost in the same fashion at the long times. Dissolution curves for film samples dissolved in

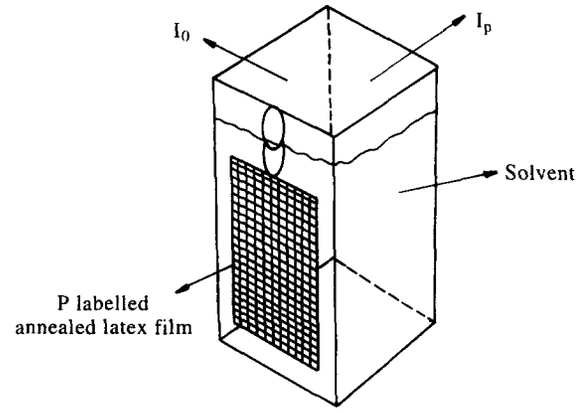

Figure 2 Dissolution cell in Ls-50 Perkin Elmer spectrofluorimeter; I_0 and I_p are the excitation and emission intensities at 345 and 375 nm, respectively

toluene/heptane (4/1) mixtures, which show a similar time dependent behaviour, are presented in *Figure 5* for various temperatures. Here, one has to note that the dissolution curves in *Figure 5* are much smoother than the curves in *Figure 4* at high temperatures, which can be explained by the slowing down effect of heptane during dissolution. In other words, dissolution can be controlled by heptane.

In order to quantify the dissolution curves, we aimed to fit the data to equation (1). *Figures 6a–c* present the plot of the following relation, for film samples dissolved in toluene at 15, 20 and 40°C temperatures, respectively:

$$\ln(1 - I_p/I_{p\infty}) = B - At \qquad (7)$$

This is the logarithmic form of equation (1) for $n = 0$ with $A = D\pi^2/d^2$ and $B = (8/\pi^2)$ parameters. Here, it is assumed that I_p is proportional to the number of P-labelled chains desorbing from the latex film, and $I_{p\infty}$ represents its value at the equilibrium condition. In *Figure 6* all dissolution curves are digitized for numerical treatment. There, one can observe the deviation from linearity at early times. Deviations from linearity in *Figures 6b* and *6c* at long times represent equilibration of the dissolution process. These results suggest that there are at least two different mechanisms involved during dissolution of annealed high-T latex films. This has already been discussed in the theoretical section. Linear regions of the curves at intermediate times in *Figure 6* follow the Fickian diffusion model where the starting point shifts to shorter times for the samples dissolved at higher temperatures. When the linear portions of the curves in *Figure 6* are compared to computations using equation (7), chain desorption coefficients, D, are obtained. The linear fit of equation (7) to the data is presented in *Figures 6a–c*. The D values obtained are listed in *Table 1*. D values, for the films dissolved in toluene, are found to be much larger at high temperatures, which is expected from the Arrhenius behaviour of

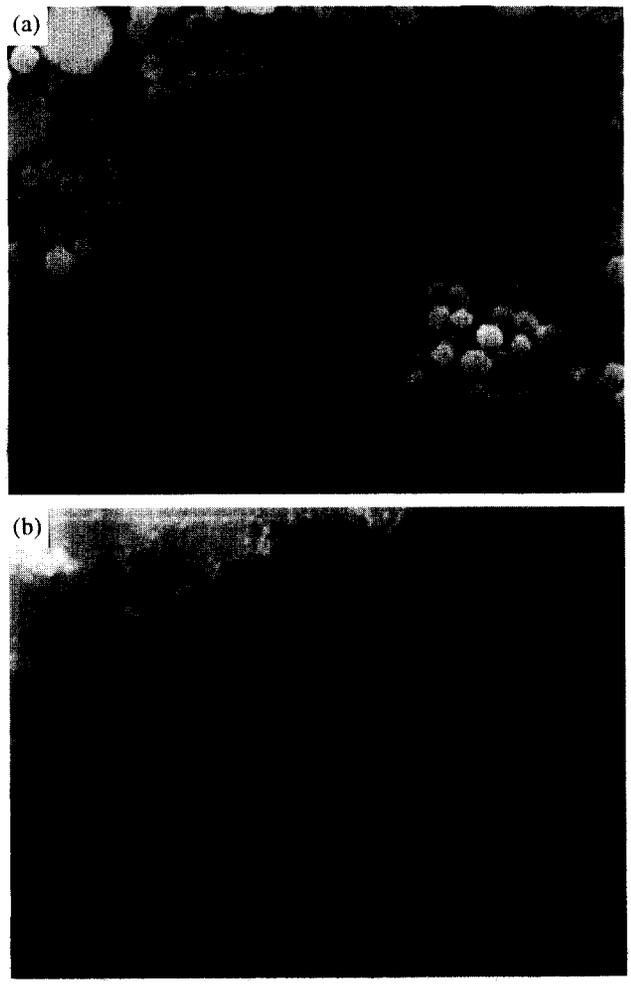

Figure 3 Scanning electron micrographs of latex film: (a) before and (b) after annealing at 180°C for 1 h

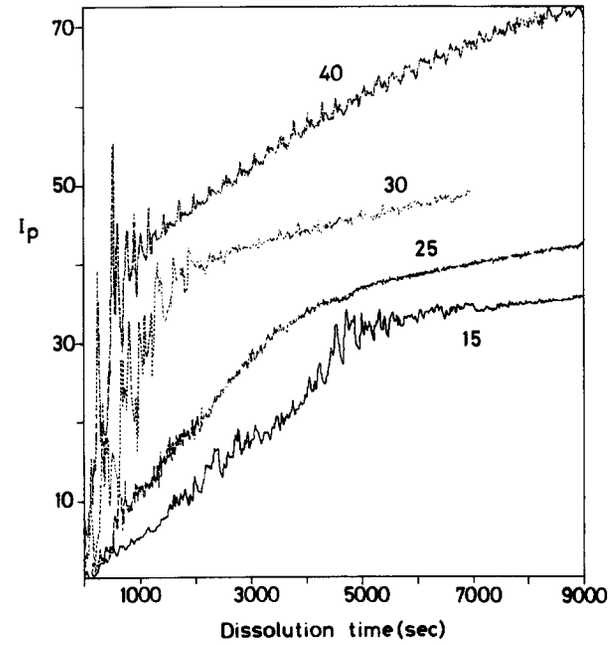

Figure 4 Pyrene intensity, I_p, *versus* dissolution time for the film samples dissolved at 15, 25, 30 and 40°C in toluene,. The cell was illuminated at 345 nm during fluorescence measurements. Data for the plot were obtained using the time drive mode of the spectrofluorimeter

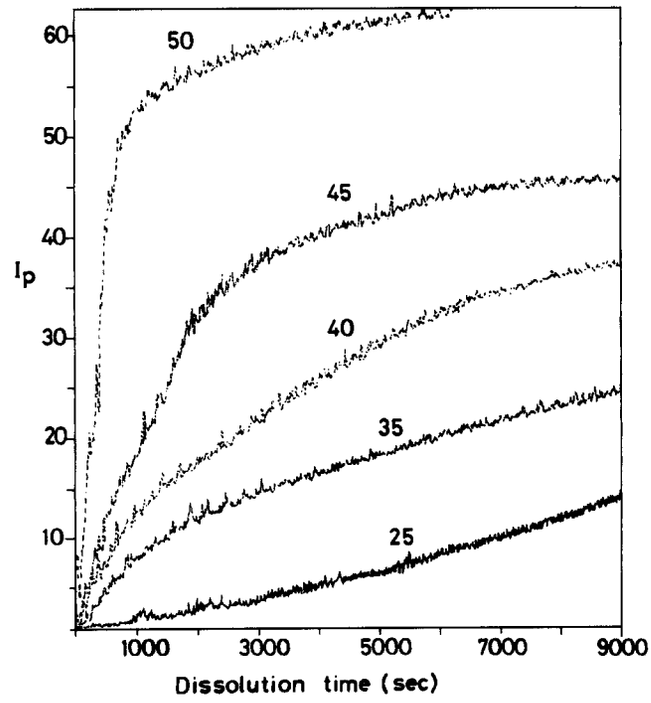

Figure 5 Pyrene intensity, I_p, *versus* dissolution time for the film samples dissolved at 25, 35, 45 and 50°C in toluene/heptane (4/1) mixtures. Data were obtained similarly to those in *Figure 4*

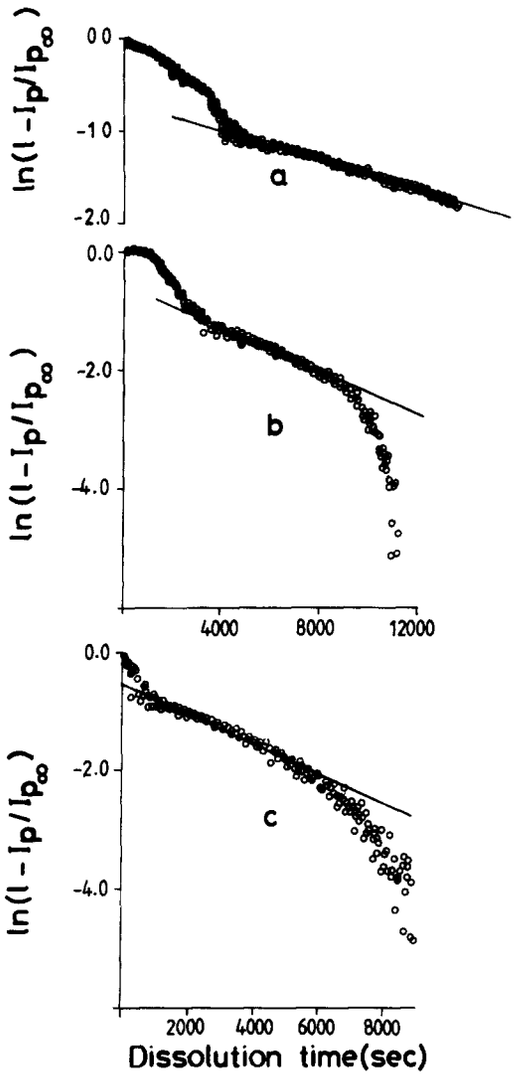

Figure 6 Plot of the digitized data in *Figure 4*, which obey the relation $\ln(1 - I_p/I_{p\infty}) = B - At$, where t is the dissolution time, and (a), (b) and (c) show the data for samples dissolved 15, 20 and 40°C, respectively. A comparison of the data in the intermediate time region is also presented with the computations obtained using equation (7). Desorption coefficients, D, are obtained from the slopes of the plots

Table 1 Experimentally obtained diffusion (D) and relaxation (k_0) parameters during dissolution of latex films in toluene at various temperatures

T (°C)	d (cm) $\times 10^{-4}$	D ($cm^2 s^{-1}$) $\times 10^{-11}$	k_0 ($mg\,cm^{-2}\,min^{-1}$) $\times 10^{-2}$
15	7.98	0.49	0.636
20	8.96	1.51	1.550
25	8.18	2.80	—
30	10.50	4.16	2.199
35	10.92	3.72	3.466
40	11.20	3.56	3.388

D. When one compares the observed $D \approx 10^{-11}\,cm^2\,s^{-1}$ values with the backbone diffusion coefficient of the interdiffusing polymer chains during film formation from PMMA latex particles[29,30] ($\approx 10^{-16}$–$10^{-14}\,cm^2\,s^{-1}$), five to three orders of magnitude difference can be seen. This is reasonable for the chains desorbing from swollen gel, during dissolution of PMMA latex films. In fact, $10^{-11}\,cm^2\,s^{-1}$ is three orders of magnitude smaller than the D values obtained for oxygen diffusing into PMMA spheres[31]. This may suggest that penetration of toluene

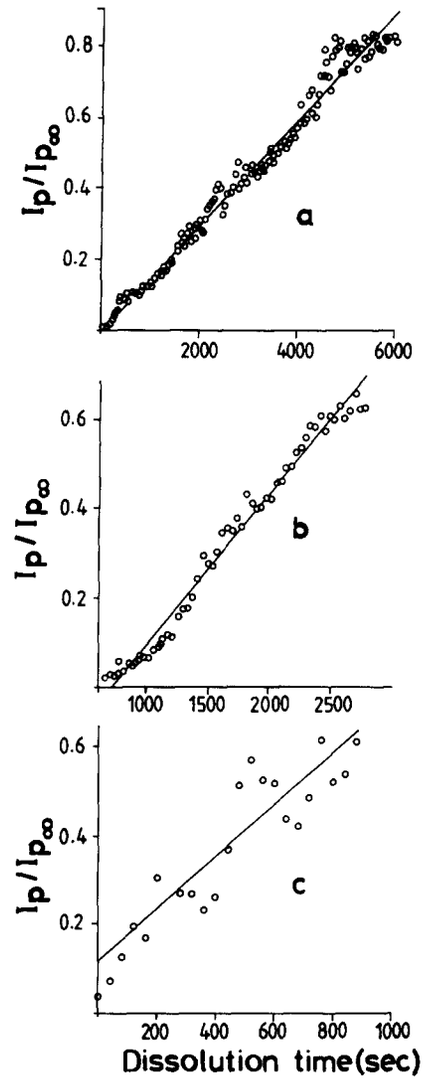

Figure 7 Comparison of the early times region of the data presented in *Figures 6a–c* with the computations obtained using equation (8). Relaxation constants, k_0, are obtained from the slopes of the plots in (a), (b) and (c) for the films dissolved at 15, 20 and 40°C, respectively

molecules into a latex film is almost as fast as desorption of PMMA chains from a swollen gel. Here, one should realize that toluene molecules are much larger in size than oxygen molecules. Our D values ($10^{-11}\,cm^2\,s^{-1}$) are also similar to the D values ($10^{-11}\,cm^2\,s^{-1}$) obtained for n-hexane desorption from polystyrene spheres[22].

Short time, non-Fickian regions of the curves in *Figure 6* are expanded and plotted in *Figures 7a–c* for the films dissolved in toluene at 15, 20 and 40°C, respectively. $I_p/I_{p\infty}$ plotted as a function of dissolution time, t, allowed a quite reasonable linear fit in this region. If we assume that the amount of penetrant toluene is proportional to the number of PMMA chains desorbing from the swollen gel, than equation (6) can be written as

$$I_p/I_{p\infty} = \frac{k_0}{C_0 d} t \qquad (8)$$

Fitting equation (8) to the data presented in *Figure 7* yielded k_0 parameters. Using known d and C_0 (0.86 $g\,ml^{-1}$) values, k_0 parameters were obtained in this set of experiments (*Table 1*). The k_0 values varied between 0.63×10^{-2} and $3.38 \times 10^{-2}\,mg\,cm^{-2}\,min^{-1}$. Again, k_0 values for samples dissolved in toluene at high temperature were found to be larger than they were at low

temperature. Our measurements of k_0 resulted in values three orders of magnitude different from those of Enscore *et al.*[22] and Jacques and Hopfenberg[32]. Thus, for n-hexane sorption by polystyrene spheres and film they reported k_0 around 10^{-5} mg cm^{-2} min^{-1}. This difference can be caused by the stronger good solvent–polymer interaction in our toluene–PMMA system. In this work, both D and k_0 values are found to be an order of magnitude smaller than they were in our previous work[13] where we used a chloroform/heptane mixture as dissolution agent. This difference can be explained by the solubility parameters of toluene [8.9 (cal cm^{-3})$^{1/2}$] and chloroform [9.3 (cal cm^{-3})$^{1/2}$], where the latter is very close to that of PMMA [9.3 (cal cm^{-3})$^{1/2}$], i.e. chloroform is a better solvent than toluene for PMMA.

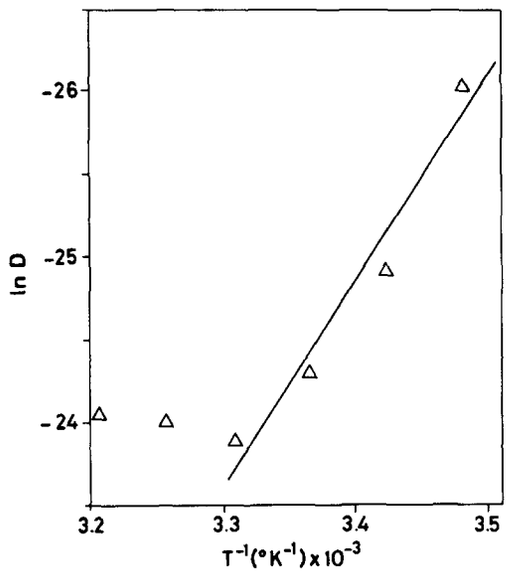

Figure 8 Plot of the logarithmic form of equation (9) for the data in *Table 1*; $\Delta E_D = 24.38$ kcal mol^{-1} is obtained from the slope of the straight line

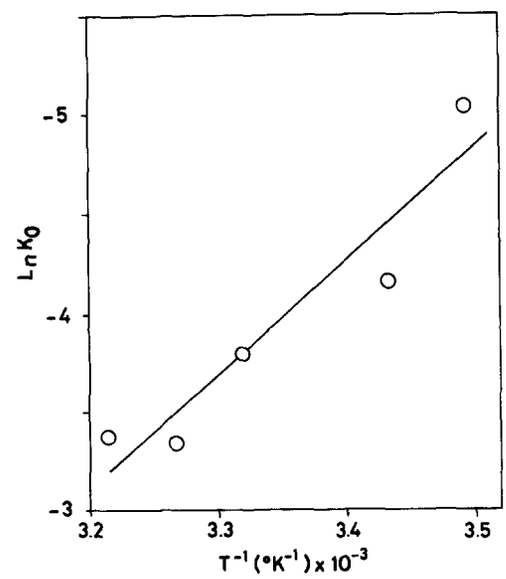

Figure 9 Plot of the logarithmic form of equation (10) for the data in *Table 1*; $\Delta E_{k0} = 11.36$ kcal mol^{-1} is obtained from the slope of the straight line

Activation energies

The temperature dependence of D and k_0 values can be interpreted by assuming that both case I and case II diffusions obey the Arrhenius relation as follows:

$$D = D' \exp\left(-\frac{\Delta E_D}{kT}\right) \tag{9}$$

and

$$k_0 = k_0' \exp\left(-\frac{\Delta E_{k_0}}{kT}\right) \tag{10}$$

here, k is the Boltzmann constant, D' and k_0' are pre-exponential factors, and ΔE_D and ΔE_{k0} are the activation energies of case I and case II diffusions, respectively. Using *Table 1*, ΔE_D and ΔE_{k0} values are produced from equations (9) and (10), which are found to be 24.38 and 11.36 kcal mol^{-1}, respectively. Arrhenius plots for D and k_0 *versus* T^{-1} are given in *Figures 8* and *9*, respectively, where it can be seen that high temperature D values are excluded from the linear fit. Here, we have to note that experimental resolution to obtain D values at high temperature is quite poor during dissolution of films in pure toluene.

Similar dissolution behaviours were observed for the

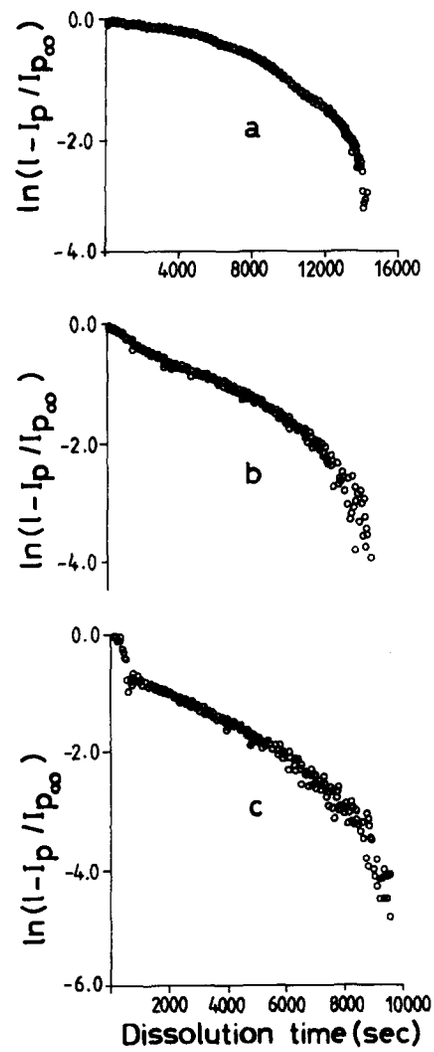

Figure 10 Plot of the digitized data of *Figure 5*, which obey the relation $\ln(1 - I_p/I_{p\infty}) = B - At$, where t is the dissolution time; (a), (b) and (c) show the data for samples dissolved at 25, 35 and 45°C respectively

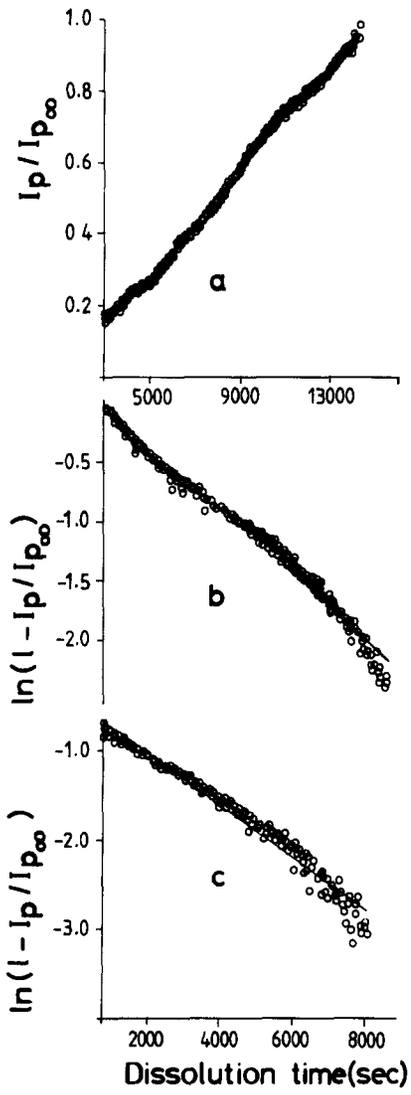

Figure 11 Comparison of the linear portions of the data presented in *Figure 10* with the computation (a) using equation (8), and (b) and (c) using equation (7). Relaxation (k_0) and diffusion constants (D) are obtained from the slopes of the plots in (a), (b) and (c) for the films dissolved at 25, 35 and 45°C, respectively

film samples dissolved in toluene/heptane mixtures. Dissolution curves in *Figure 5* of this set of experiments are digitized according to equation (7) for numerical treatment and are plotted in *Figure 10*. *Figure 10a* presents the curve for the film sample dissolved at 25°C, which shows pure case II behaviour. However, curves in *Figures 10b* and *c* present case I characteristics. Data in *Figure 10a* are fitted to equation (8) in *Figure 11a* where k_0 is obtained. Data in *Figure 10b* and *c* are fitted to equation (7) to produce D values in *Figures 11b* and *c*, respectively. Experimentally obtained D and k_0 values are given in *Table 2*, where k_0 values for high temperatures are missing due to the pure Fickian behaviour of these dissolution processes. At 25 and 30 °C, due to pure case II behaviour, D values could not be produced. The k_0 and D values for the dissolution in toluene were found to be larger than they are in the toluene/heptane mixture, which is understandable due to the high solubility of PMMA in pure toluene.

Using *Table 2* and equation (9), diffusion activation energy ΔE_D was calculated and found to be 24.41 kcal mol^{-1}. An Arrhenius plot for D is presented in *Figure 12*. The ΔE_D values obtained from both sets of

Table 2 Experimentally obtained diffusion (D) and relaxation (k_0) parameters during dissolution of latex films in toluene/heptane mixtures at various temperatures

T (°C)	d (cm) $\times 10^{-4}$	D (cm^2 s^{-1}) $\times 10^{-11}$	k_0 (mg cm^{-2} min^{-1}) $\times 10^{-2}$
25	11.20	—	0.412
30	9.05	—	0.378
35	10.50	2.40	—
40	9.66	2.26	—
45	9.24	2.92	—
50	9.24	4.53	—
55	10.08	7.90	—
60	10.76	26.50	—
65	9.24	32.40	—

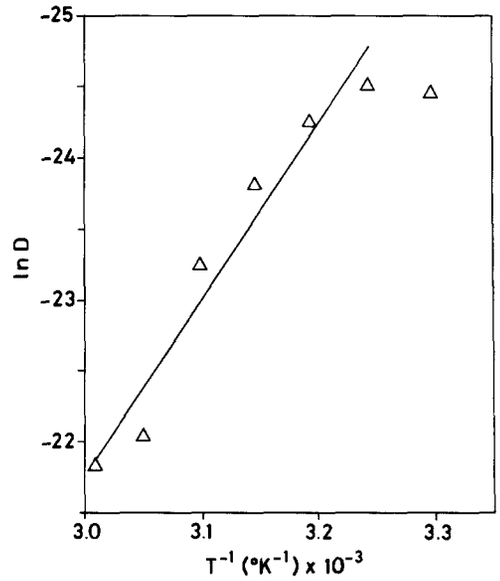

Figure 12 Plot of the logarithmic form of equation (9) for the data in *Table 2*; $\Delta E_D = 24.41$ kcal mol^{-1} is obtained from the slope of the straight line

experiments are very close to each other, and the magnitude is quite close to the energy characteristic of a polymer chain backbone motion[23,33]. The magnitude of observed ΔE_{k0} energy is much smaller than ΔE_D energies and very close to that typically observed for side-chain motion for PMMA[23,27,33,34]. From here we can reach a conclusion that during dissolution processes, after creation of the gel layer, polymer chains disentangle with the help of their side chain motion and then diffuse into the solvent reservoir by their translational backbone motion.

ACKNOWLEDGEMENT

We thank Professor M. A. Winnik for supplying us with the latex material and documents to read.

REFERENCES

1. Crank, J., *The Mathematics of Diffusion*. Clarendon Press, Oxford, UK, 1975, pp. 26–41.
2. Ueberreiter, K., in *Diffusion in Polymers*, ed. J. Crank and G. S. Park. Academic Press, London, 1968, pp. 220–257.
3. Quano, A. C. and Carothers, J. A., *Polym. Eng. Sci.*, 1980, **20**, 160.
4. Krasicky, P. D., Groele, R. J. and Rodriguez, F., *J. Appl. Polym. Sci.*, 1988, **35**, 641.

5. Limm, W., Dimnik, G. D., Stanton, D., Winnik, M. A. and Smith, B. A., *J. Appl. Polym. Sci.*, 1988, **35**, 2099.
6. Guillet, J. E., in *Photophysical and Photochemical Tools in Polymer Science*, ed. M. A. Winnik. Reidel, Dordrecht, The Netherlands, 1986, pp. 467–492.
7. Nivaggioli, T., Wang, F. and Winnik, M. A., *J. Phys. Chem* 1992, **96**, 7462.
8. Pascal, D., Duhamel, J., Wang, Y., Winnik, M. A., Napper, D. H. and Gilbert, R., *Polymer*, 1993, **34**, 1134.
9. Lu, L. and Weiss, R. G., *Macromolecules*, 1994, **27**, 219.
10. Krongauz, V. V., Mooney III, W. F., Palmer, J. W. and Patricia, J. J., *J. Appl. Polym. Sci.*, 1995, **56**, 1077.
11. Krongauz, V. V. and Yohannan, R. M., *Polymer*, 1990, **31**, 1130.
12. He, Z., Hammond, G. S. and Weiss, R. G., *Macromolecules*, 1992, **25**, 501.
13. Pekcan, Ö., Canpolat, M. and Kaya, D., *J. Appl. Polym. Sci.*, 1996, **60**, 2105.
14. Pekcan, Ö., Uğur, Ş. and Yilmaz, Y., *Polymer* (in press).
15. Winnik, M. A., Hua, M. H., Hongham, B., Williamson, B. and Croucher, M. D., *Macromolecules*, 1984, **17**, 262.
16. Pekcan, Ö., Winnik, M. A. and Croucher, M. D., *Phys. Rev. Lett.*, 1988, **61**, 641.
17. Pekcan, Ö., *Chem. Phys. Lett.*, 1992, **20**, 198.
18. Tu, Y. O. and Quano, A. C., *IBM J. Res. Dev.*, 1977, **21**, 131.
19. Lee, P. I. and Peppas, N. A., *J. Controlled Release*, 1987, **6**, 207.
20. Brochardt, F. and de Gennes, P. G., *Physico-Chem. Hydrodynamics*, 1983, **4**, 313.
21. Papanu, J. S., Soane, D. S. and Bell, A. T., *J. Appl. Polym. Sci.*, 1989, **38**, 859.
22. Enscore, D. J., Hopfenberg, H. B. and Stannett, V. T., *Polymer*, 1977, **18**, 793.
23. Canpolat, M. and Pekcan, Ö., *Polymer*, 1995, **36**, 2025.
24. Pekcan, Ö., *Trends Polym. Sci.*, 1994, **2**, 236.
25. Canpolat, M. and Pekcan, Ö., *J. Appl. Polym. Sci.*, 1996, **59**, 11.
26. Pekcan, Ö. and Canpolat, M., *J. Appl. Polym. Sci*, 1996, **59**, 277.
27. Canpolat, M. and Pekcan, Ö., *J. Polym. Sci., Polym. Phys. Ed.*, 1996, **34**, 691.
28. Canpolat, M. and Pekcan, Ö., *Polymer*, 1995, **36**, 4433.
29. Winnik, M. A., Pekcan, Ö. and Croucher, M. D., in *Scientific Methods for the Study of Polymer Colloids and their Applications*, ed. F. Candau and R. H. Ottewill. NATO, ASI, Kluwer Academic. London, Boston, Dordrecht, 1988, pp. 225–246.
30. Pekcan, Ö., Winnik, M. A. and Croucher, M. D., *Macromolecules*, 1990, **23**, 2673.
31. Kaptan, Y., Pekcan, Ö. and Güven, O., *J. Appl. Polym. Sci.*, 1992, **44**, 1595.
32. Jacques, C. H. M. and Hopfenberg, H. B., *Polym. Eng. Sci.*, 1974, **14**, 449.
33. Shiotani, M. and Sohma, J., *Polymer J.*, 1977, **9**, 283.
34. Shiotani, M., Sohma, J. and Freed, J. H., *Macromolecules*, 1983, **16**, 1495.